

Transition-Metal Complexes with the Novel Scorpionate Ligand Dihydrobis-(tetrazolyl)borate: Synthesis and Characterization of Infinite Two-Dimensional Metal-Ligand Frameworks and One-Dimensional Water Substructures[☆]

Christoph Janiak^{*a}, Tobias G. Scharmann^a, Klaus-Werner Brzezinka^b, and Peter Reich^b

Institut für Anorganische und Analytische Chemie, Technische Universität Berlin^a,
Straße des 17. Juni 135, 10623 Berlin, Germany

Bundesanstalt für Materialprüfung und -forschung (BAM)^b,
Unter den Eichen 87, 12205 Berlin, Germany

Received October 13, 1994

Key Words: Poly(azolyl)borates, metal complexes of / Bis(tetrazolyl)borate, metal complexes of / Metal-nitrogen coordination / Coordination polymers

Dihydrobis(tetrazolyl)borate metal compounds of the composition $[M(L)_2\{\mu\text{-H}_2\text{B}(\text{CHN}_4)_2\}_2]_n$ for $M = \text{Mn, Fe, Co, Zn, Cd}$ with $L = \text{H}_2\text{O}$ and for $M = \text{Cu}$ with $L = \text{NH}_3$ are obtained from metal salts and $\text{K}[\text{H}_2\text{B}(\text{CHN}_4)_2]$. Single-crystal X-ray studies reveal the formation of two-dimensional rhombic grid sheets through the bridging action of the bis(tetrazolyl)borate ligands. Each metal atom is octahedrally coordinated with two *trans* L ligands and four $\text{H}_2\text{B}(\text{CHN}_4)_2$ nitrogen do-

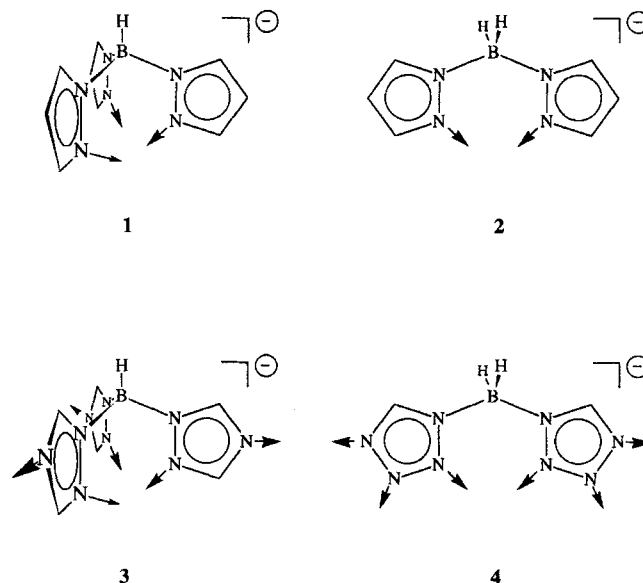
minors. Two additional, hydrogen-bonded water molecules occupy the rhombic openings in the compounds with $M = \text{Mn, Fe, Co, Zn, and Cd}$. The water of crystallization is held in place through hydrogen bonding from the water ligands and to the nitrogen atoms to give a substructure of parallel kinked water chains. Temperature-variable magnetic measurements show a Curie-Weiss behavior for the paramagnetic complexes with $M = \text{Mn, Fe, Co, and Cu}$.

Our research is concerned with modifications of the scorpionate or poly(pyrazolyl)borate ligands **1** and **2**^[1], such that the pyrazolyl rings are replaced by 1,2,4-triazolyl or tetrazolyl rings, for example. The resulting ambidentate poly-triazolyl- and -tetrazolyl-borate anions, e. g. $[\text{HB}(\text{C}_2\text{H}_2\text{N}_3)_3]^-$ (**3**)^[2-4] and $[\text{H}_2\text{B}(\text{CHN}_4)_2]^-$ (**4**)^[5] with their multiple bonding centers give rise to an interesting coordination chemistry and supramolecular architecture in the solid state with the formation of incorporated two-dimensional water layers^[6] and linkage isomerism^[7] for **3** and the formation of two-dimensional rhombic grid sheets for **4**^[6]. The controlled synthesis of two- and three-dimensional inorganic materials with inner cavities for the catalysis of organic reactions^[8] or with collective magnetic phenomena for the design of molecular based ferromagnets^[9] is receiving an increased attention^[10].

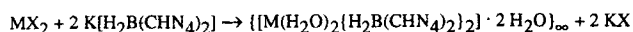
In this paper we report on the synthesis of two-dimensional coordination polymers from **4** with manganese(II), iron(II), cobalt(II), copper(II), zinc(II), and cadmium(II) cations, their magnetic properties and the results of single crystal X-ray studies.

Syntheses and Properties of $\{[M(\text{H}_2\text{O})_2\{\mu\text{-H}_2\text{B}(\text{CHN}_4)_2\}_2] \cdot 2 \text{H}_2\text{O}\}_\infty$ for $M = \text{Mn}$ (5**), Fe (**6**), Co (**7**), Zn (**9**), and Cd (**10**), and of $\{\text{Cu}(\text{NH}_3)_2\{\mu\text{-H}_2\text{B}(\text{CHN}_4)_2\}_2\}_\infty$ (**8**)**

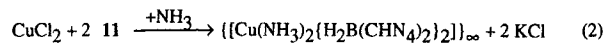
The dihydrobis(tetrazolyl)borate anion **4** in the form of its potassium salt (**11**) reacts with manganese(II), cobalt(II), and cadmium(II) chloride, iron(II) sulfate, as well as with zinc(II) acetate in water to form the diaquabis[μ -dihydrobis-(tetrazolyl)borate]metal(II) complexes **5–7**, **9**, **10** (eq. 1).



Upon slow diffusion of solutions of the reactants the iron, cobalt, zinc and cadmium complexes together with water of crystallization are obtained as colorless (**6**, **9**, **10**) and orange (**7**) crystals directly from the reaction mixture in 35–57% crystal yield. The analogous manganese compound (**5**) is formed when the water is allowed to slowly evaporate at room temperature at normal pressure. From the resulting crystal mixture, the colorless crystals of **5** are obtained in analytically pure form upon washing with water to remove the cocrystallized unreacted starting material and potassium chloride.



11		M	X	(1)
	5	Mn	Cl	
	6	Fe	(SO ₄) _{1/2}	
	7	Co	Cl	
	9	Zn	O ₂ CCH ₃	
	10	Cd	Cl	



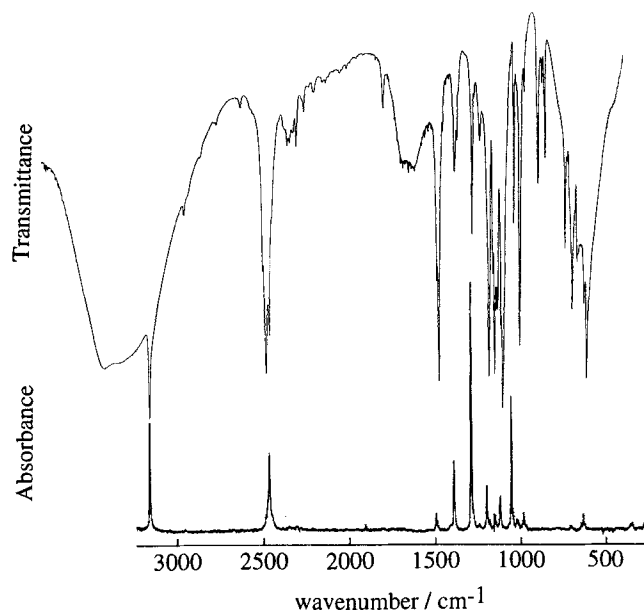
8

The copper complex **8** is initially obtained as a dark blue amorphous precipitate in water. While the bis(tetrazolyl)borato metal complexes are insoluble in water or organic solvents once they have formed and, thus, cannot be recrystallized, the copper compound can be redissolved in aqueous ammonia solution (eq. 2) from which it precipitates upon slow solvent evaporation as blue-violet crystals. Presumably, this recrystallization has been successful because of the availability of a stable metal-ammine complex in the form of tetraamminecopper. The crystallization of the copper complex is not without difficulties, however, since a white, a turquoise, and a light blue microcrystalline material are formed together with the actual blue-violet complex. Vibrational spectroscopic studies suggest that they also contain the bis(tetrazolyl)borate moiety, but their exact composition or structure could not be elucidated. In the course of the formation of **6**, **7** and **9** gas evolution takes place which is interpreted (vide infra) as being due to hydrogen formation from a partial hydrolysis of **4**. Hydronium ions (from the transition metal cation acids) can react with the boron-bonded hydridic hydrogens.

X-ray structural investigations show that the crystals of **5–7** and **9, 10** contain two molecules of hydrogen-bonded water of crystallization per formula unit aside from the metal-coordinated aqua ligands. This solvent of crystallization is not or only very slowly lost over a several-month period when the air-dried crystals are stored at room temperature. Heating of the crystalline material leads to loss of water of crystallization at around 100°C with the retention of the crystalline shape. Most of the compounds appear to be infusible materials up to over 260 or even 350°C, except for the cobalt complex **7** and the copper compound **8**. Decomposition of **7** becomes clearly visible at 280°C. Monitoring the heating process for **7** (in air) with a thermogravimetric balance, however, shows the onset of decomposition at about 200°C, followed by a slow but steady weight loss of altogether 58% up to 800°C. *Care should however be taken when heating the materials over 190°C because explosive decompositions have in some cases been observed above this temperature:* When a sample of the cobalt compound was heated in an argon atmosphere at normal pressure an explosive decomposition occurred at 197°C. The same happened at 210°C when heating a sample of the copper complex **8** in air. The cadmium complex **10** could normally be heated over 350°C without problems, yet in two cases it also explosively decomposed at 250°C. These observations

suggest that the thermal behavior of the other derivatives **5**, **6**, and **9** may also be unpredictable above ca. 200°C. The vibrational spectra (infrared and Raman) of the complexes are essentially similar in the measured wave number range (400–4000 cm⁻¹ for the IR and 40–3250 cm⁻¹ for the Raman spectra). Typical characteristic bands are observed, e. g., at 2450 (νB–H) and 3150 cm⁻¹ (νC–H for the tetrazolyl ring). It seems, that a band at 1285 cm⁻¹ with the highest intensity in the Raman spectra and weak intensity in the IR spectra of all complexes is the “breathing” vibration of the tetrazolyl ring. Typical spectra are displayed in Figure 1.

Figure 1. Typical infrared (top) and Raman spectrum (bottom) for the dihydrobis(tetrazolyl)borate metal compounds (spectra collected with the zinc complex **9**)



X-Ray Structure Analyses of **5–10**

The formation of a two-dimensional coordination polymer has been observed so far as the only structural motif in the transition metal complexes of **4**. The arrangement of the metal centers and ligands within such a layer is illustrated in Figure 2 for the isomorphous structures of **5–7** and **9, 10**. The relative packing of these layers together with their kinked nature can be visualized from a stereo plot provided in Figure 3. Figure 4 shows the Jahn-Teller-distorted layer polymer for the copper complex **8**. The distorted copper complex **8** exhibits the expected four short and two long Cu–N distances. The elongation of two bonds to tetrazolyl nitrogen atoms is the origin of the observed layer distortion. The metal centers in **5–10** are in all cases octahedrally coordinated, with the coordination polyhedron being formed from four nitrogen atoms of the bis(tetrazolyl)borate ligands and two *trans*-coordinated solvate molecules (H₂O in **5–7** and **9, 10**; NH₃ in **8**). The metal coordination and atomic numbering scheme are depicted in Figure 5. Only the C–H neighboring N-4 atom functions as a donor atom to the metal center, in agreement with the

charge distribution from an AM1 calculation which assigns the highest negative charge and electrostatic potential to this nitrogen^[6]. Thus, in contrast to the bidentate dihydrobis(*pyrazolyl*)borate ligand **2**^[1], the dihydrobis(*tetrazolyl*)borate ligand **4** does not form chelates but bridges between metal atoms. Selected bond lengths and angles are collected in Table 1. A plot of the M–N and M–O distances versus M, given in Figure 6, shows the expected decrease for high-spin ions from Mn to Co, with a minimum at Ni (not investigated here) and again an increase towards Zn^[13].

Figure 2. Structure of the two-dimensional metal-ligand grid sheets in the isomorphous complexes **5–7, 9, and 10** (PLUTON plot^[12])

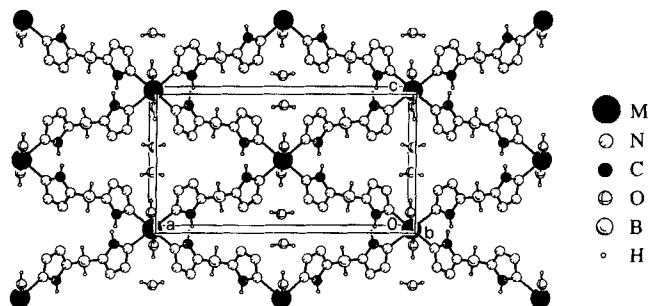


Figure 3. Stereo plot for the crystal packing of the grid sheets in **5–7, 9, and 10** (PLUTON^[12])

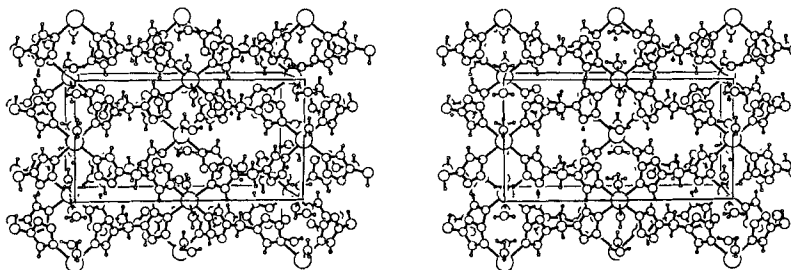
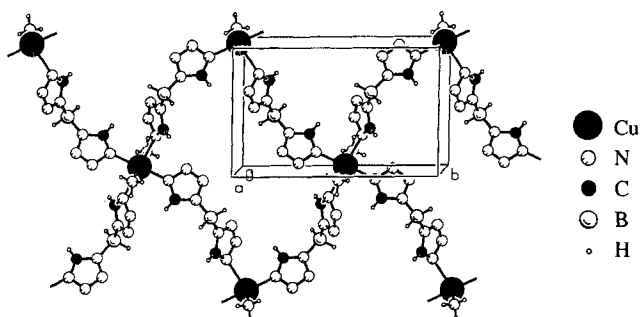
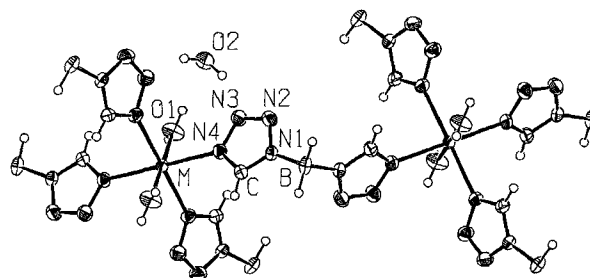


Figure 4. Structure of the Jahn-Teller-distorted two-dimensional Cu-ligand framework in **8** (PLUTON^[12])



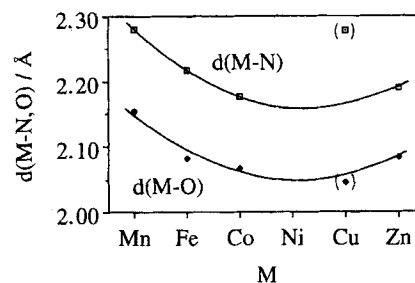
The rhombohedral openings in the undistorted coordination polymers **5–7 and 9, 10** are filled with two water molecules of crystallization, which have fully been localized including the hydrogen atoms (Figure 2). These water molecules are held tightly in place through hydrogen bonding to the N-3 atoms of the tetrazolyl rings ($O-(H)\cdots N = 2.84 \pm 0.03 \text{ \AA}$) and by means of the metal-coordinated water ligands. The aqua ligand forms two hydrogen bonds, one

Figure 5. Detailed metal coordination and atomic numbering scheme in the isomorphous complexes **5–7, 9, and 10** (PLATON-TME plot^[12])



to each of the adjacent water of crystallization [$O-(H)\cdots O = 2.68 \pm 0.02$ and $2.855 \pm 0.004 \text{ \AA}$], thus giving rise to one-dimensional chains of water molecules which run parallel to the two-dimensional metal-ligand grid sheets (Figure 7). The variances in the above hydrogen bonds cover the ranges observed in the different metal complexes **5–7, 9, and 10**. It is evident that there is essentially no variation with the change in the metal. The parameters for the individual hydrogen schemes of each complex are included in Table 1. The stereo plot in Figure 3 reveals that the rhombohedral, water-filled openings do not extend

Figure 6. Variation of the M–N and M–O distances with the metal (d-electron configuration respectively) in **5–9**. For the Jahn-Teller-distorted Cu complex **8** both the long and short Cu–N distances are given



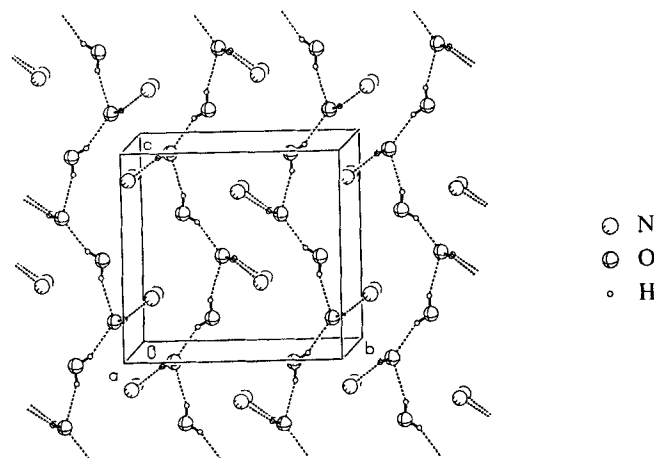
through the crystal lattice as open channels since the next layers are shifted half a unit cell along *a* so that caves are formed. The formation of two- and three-dimensional coordination polymers has recently also been discussed under the terms of self-assembly of molecular building blocks^[11].

The B–N, C–N, and N–N bond lengths and angles in the tetrazolylborate moiety (cf. Table 1) are similar to those observed in bis- or tris(*pyrazolyl*)borate ligands^[1,14], tetra-

Table 1. Selected bond lengths [Å] and angles [°] for **5–10** including the hydrogen bonding network (cf. Figure 5 for the atomic numbering scheme). Symmetry transformations: f: $-0.5 - x, y, 0.5 - z$; g: $-x, 0.5 - y, -0.5 + z$

Compound	5 (M = Mn)	6 (M = Fe)	7 (M = Co)	8 (M = Cu) [a]	9 (M = Zn)	10 (M = Cd)
M - N	2.281(2)	2.218(1)	2.176(2)	2.045(3), 2.512(4)	2.190(3)	2.358(2)
M - O (solvate ligand)	2.154(3)	2.083(2)	2.067(2)	2.021(4)	2.085(3)	2.272(3)
B - N1	1.566(3)	1.567(2)	1.568(2)	1.554(5), 1.571(5)	1.572(4)	1.574(3)
N1 - N2	1.347(3)	1.342(2)	1.349(2)	1.343(4), 1.353(4)	1.348(4)	1.340(3)
N2 - N3	1.295(3)	1.292(2)	1.296(2)	1.291(4), 1.296(4)	1.299(4)	1.299(3)
N3 - N4	1.355(3)	1.353(2)	1.353(2)	1.334(4), 1.354(4)	1.358(4)	1.355(3)
N4 - C	1.316(3)	1.315(2)	1.316(2)	1.309(5), 1.311(4)	1.308(5)	1.312(3)
C - N1	1.321(3)	1.318(2)	1.317(2)	1.322(5), 1.318(4)	1.319(5)	1.325(3)
O - M - N (NH ₃ -Cu-N)	90.94(7), 89.06(7)	91.55(5), 88.45(5)	90.97(5), 89.03(5)	89.2(1), 90.8(1) 88.3(1), 91.7(1)	91.2(1), 88.8(1)	90.88(7), 89.12(7)
cis N - M - N	88.36(6), 91.64(6)	88.20(5), 91.80(5)	89.59(5), 90.41(5)	86.6(1), 93.4(1)	88.7(1), 91.3(1)	88.01(6), 91.99(6)
N1 - B - N1f	106.0(3)	106.3(1)	106.3(2)	109.6(3)	105.9(3)	106.0(3)
hydrogen bonding scheme:						
O1...O2(g)	2.683(4), 2.855(5)	2.695(3), 2.851(3)	2.666(3), 2.859(3)	--	2.666(5), 2.855(5)	2.704(4), 2.855(4)
O1-H...O2(g)	157(3), 159(3)	158(3), 158(3)	157(4), 164(3)	--	152(6), 152(6)	155(4), 164(4)
O2...N3	2.840(3)	2.819(2)	2.820(3)	--	2.819(4)	2.877(3)
O2-H...N3	155(2)	155(2)	153(2)	--	124(4)	164(3)
shortest M...M separations:	6.977(5), 9.543(7)	6.956(2), 9.444(3)	6.984(4), 9.435(5)	7.653(3), 8.170(3)	6.973(3), 9.444(4)	7.023(3), 9.650(3)

[a] The two tetrazolyl rings are not symmetry-related in the structure of the copper complex **8**, thus giving rise to two sets of distances and NH₃-Cu-N angles.

Figure 7. Water substructure and hydrogen bonding network in the isomorphous complexes **5–7**, **9**, and **10** (PLUTON^[12])

zolate complexes^[15], or the potassium salt of **4**^[5]. As in the structures of the latter two, the “inner” N–N bond N2–N3 remains shorter by 0.04–5 Å than the neighboring N–N bonds.

Magnetic Properties of **5–8**

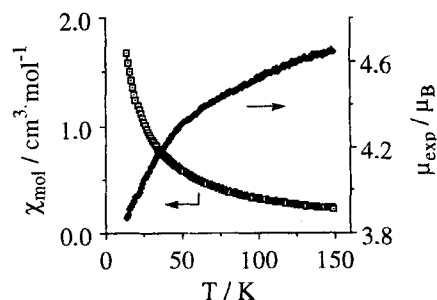
The magnetic data for **5–8** is listed in Table 2. Temperature-variable magnetic measurements confirm the manganese, iron, and cobalt compound to be high-spin complexes. The magnetic moments lie within the range typically observed for complexes of the respective transition metal. The variations of the susceptibility for **5–8** with temperature are characteristic of normal paramagnets in the temperature range measured (12–308 K for **5–7**, 80–320 K for **8**), and the Curie-Weiss law is obeyed. Thus, there is neither a magnetic coupling transmitted through the ligand nor a through-space interaction of the metal centers (shortest M–M contacts about 6.97 Å for **5–7** and 7.65 Å for **8**).

The magnetic moments listed in Table 2 are temperature-independent within experimental error, except for **7**, where μ depends on temperature. This situation is illustrated in Figure 8 and is due to the fact that the ground term is degenerate, and there are thermally accessible degenerated excited terms^[17].

Table 2. Magnetochemical data for **5–8**

	$\mu_{\text{exp}}/\mu_{\text{B}}$ [a]	Θ / K [b]	$\mu_{\text{s.o.}}/\mu_{\text{B}}$ [c]	$\mu_{\text{obs.}}/\mu_{\text{B}}$ [d]
5	5.8	0	5.92	5.7 - 6.0
6	5.1	8	4.90	5.1 - 5.7
7	4.7	-11	3.87	4.3 - 5.2
8	1.9	-99	1.7	1.8 - 2.1

[a] Experimentally obtained magnetic moment at 300 K. No diamagnetic correction employed. Temperature range measured: 12–308 K for **5–7**, 80–320 K for **8**. – [b] Curie-Weiss constant from a plot of $1/\chi$ against T . – [c] Calculated spin-only value $\mu_{\text{s.o.}}/\mu_{\text{B}} = 2[S(S+1)]^{1/2}$ for the free ions Mn²⁺, Fe²⁺, Co²⁺, and Cu²⁺. – [d] Typical range for observed magnetic moments in metal complexes at 300 K^[16,17].

Figure 8. Temperature variations of the molar susceptibility (χ_{mol}) and the magnetic moment (μ_{exp}) of **7** between 14 and 150 K

Conclusions

The introduction of additional nitrogen coordination centers into the bis(pyrazolyl)borate ligand **2** to give the

bis(tetrazolyl)borate ligand **4** changes the coordination chemistry from a chelate to a bridging ligand. Metal coordination and bridging action through the exodentate, CH-neighboring nitrogen atom in **4** lead to the formation of extended two-dimensional rhombic grid sheets. Each metal is coordinated by four nitrogen atoms and its coordination sphere then completed to an octahedron by two *trans* solvate molecules.

This work was supported by the *Deutsche Forschungsgemeinschaft* (grant Ja466/4-1), the *Fonds der Chemischen Industrie*, and the *Freunde der TU Berlin*. We thank Prof. H. Schumann for his generous and encouraging support, Mrs. M. Borowski and Mr. F.

Girgsdies for collecting the crystallographic data sets. The help of Dr. H. W. Sichtung and Dr. W. Günther in obtaining the magnetochemical data is appreciated.

Experimental

Bidistilled or deionized water was used as a solvent. – CHN: Perkin-Elmer Series II CHNS/O Analyzer 2400. – IR: Perkin-Elmer 580B or Nicolet Magna 750. – Raman: Carl-Zeiss-Jena ILA 120 (10 mW Ar laser, 514.5 nm, 3 mW at the sample). – Susceptibility measurements: Faraday magnetic balance and AC susceptibility meter Lakeshore Model 7000. – The potassium salt of **4** was synthesized from KBH_4 and tetrazole according to ref.^[5]

Table 3. Yields, melting points, colors, and elemental analyses for the dihydrobis(tetrazolyl)borate metal complexes **5–10**

	Formula	Mol. Mass	Yield [a]	Color	m. p. [b]	Analyses		calcd. [c] found	
						C	H	N	M
5	$\text{C}_4\text{H}_{16}\text{B}_2\text{MnN}_{16}\text{O}_4$	428.8	0.30 g (53%)	colorless	> 260 °C	11.20 11.70	3.76 3.55	52.26 52.02	12.81 n. d.
6	$\text{C}_4\text{H}_{16}\text{B}_2\text{FeN}_{16}\text{O}_4$	429.8	0.26 g (47%)	colorless	> 260 °C	11.18 11.30	3.75 3.41	52.15 49.35	13.00 n. d.
7	$\text{C}_4\text{H}_{16}\text{B}_2\text{CoN}_{16}\text{O}_4$	432.8	0.20 g (35%)	orange	200 °C (dec.)	11.10 11.15	3.73 3.41	51.78 51.50	13.62 n. d.
8	$\text{C}_4\text{H}_{16}\text{B}_2\text{CuN}_{16}\text{O}_4$	399.4	0.20 g (38%)	blue-violet	210 °C (dec)	12.02 12.72	3.53 3.46	63.12 60.25	15.91 n. d.
9	$\text{C}_4\text{H}_{16}\text{B}_2\text{N}_{16}\text{O}_4\text{Zn}$	439.3	0.33 g (57%)	colorless	(> 350 °C)	10.94 10.90	3.67 3.43	51.02 50.86	14.88 14.89
10	$\text{C}_4\text{H}_{16}\text{B}_2\text{CdN}_{16}\text{O}_4$	486.3	0.30 g (47%)	colorless	(> 350 °C) / 250 °C (dec.)	9.88 9.52	3.32 2.85	46.09 44.54	23.12 n. d.

[a] Crystalline material. – [b] The clear crystals turn blind at around 100 °C due to the loss of the water of crystallization. – [c] n.d. = not determined.

Table 4. Crystal data for the compounds **5–10**

Compound	5	6	7	8	9	10
Formula	$\text{C}_4\text{H}_{16}\text{B}_2\text{MnN}_{16}\text{O}_4$	$\text{C}_4\text{H}_{16}\text{B}_2\text{FeN}_{16}\text{O}_4$	$\text{C}_4\text{H}_{16}\text{B}_2\text{CoN}_{16}\text{O}_4$	$\text{C}_4\text{H}_{16}\text{B}_2\text{CuN}_{16}\text{O}_4$	$\text{C}_4\text{H}_{16}\text{B}_2\text{N}_{16}\text{O}_4\text{Zn}$	$\text{C}_4\text{H}_{16}\text{B}_2\text{CdN}_{16}\text{O}_4$
Mol. mass [g mol ⁻¹]	428.84	429.75	432.83	399.45	439.29	486.31
Crystal size [mm]	0.5·0.4·0.3	0.5·0.5·0.4	0.6·0.6·0.4	0.4·0.4·0.5	0.5·0.6·0.3	0.4·0.1·0.1
Temperature [K]	293	293	293	293	293	293
Crystal system	Orthorhombic	Orthorhombic	Orthorhombic	Monoclinic	Orthorhombic	Orthorhombic
Space group	<i>Cc</i> mb [a]	<i>Cc</i> mb [a]	<i>Cc</i> mb [a]	<i>P</i> 2 ₁ / <i>a</i> (No. 14)	<i>Cc</i> mb [a]	<i>Cc</i> mb [a]
Cell constants:						
<i>a</i> [Å]	18.081(7)	17.890(5)	17.682(2)	7.995(3)	17.772(3)	18.366(5)
<i>b</i> [Å]	10.180(7)	10.218(1)	10.299(5)	13.052(5)	10.261(2)	10.207(2)
<i>c</i> [Å]	9.543(7)	9.444(1)	9.435(5)	8.170(2)	9.444(4)	9.650(2)
β [°]	90	90	90	102.49(2)	90	90
<i>V</i> [Å ³]	1756(2)	1726.2(6)	1718(1)	832.4(5)	1722.0(9)	1809.1(7)
<i>Z</i>	4	4	4	2	4	4
<i>D</i> _{calc} [g cm ⁻³]	1.622	1.653	1.673	1.594	1.694	1.785
<i>F</i> (000) [electrons]	876	880	884	406	896	968
μ (MoK α) [cm ⁻¹]	7.7	9.2	10.5	13.5	15.1	12.5
Absorption correction:	DIFABS	–	DIFABS	DIFABS	DIFABS	DIFABS
max.; min.; av.	1.291; 0.950; 1.044	–	1.184; 0.956; 1.029	1.051; 0.542; 0.839	1.453; 0.843; 0.974	1.484; 0.968; 1.151
Weighting scheme: <i>k</i> , <i>g</i>	unit weights	unit weights	unit weights	1.0; 0.0	2.16; 0.0	1.98; 0.0
No. of reflections:						
measured	2355	1144	2297	2149	1946	2415
independent	996	971	1003	1774	1012	1015
observed	[>4 σ (<i>F</i>)] 815	[>2 σ (<i>F</i>)] 909	[>4 σ (<i>F</i>)] 935	[>4 σ (<i>F</i>)] 1396	[>4 σ (<i>F</i>)] 940	[>4 σ (<i>F</i>)] 876
No. of variables	85	85	85	136	85	85
<i>R</i> ; <i>R</i> _w [b]	0.0298	0.0227	0.0246	0.0395; 0.0382	0.0489; 0.0520	0.0240; 0.0230
$\Delta\rho$: max; min [e Å ⁻³]	0.26; -0.25	0.22; -0.19	0.26; -0.33	0.40; -0.62	0.66; -0.72	0.34; -0.51

[a] Non-standard setting of *Cmca* (No. 64). In ref.^[6], the structures of **7**, **9**, and **10** were erroneously reported to have been solved in the isomorphic subgroup *Ccm*2₁. – [b] $R = (\sum ||F_o| - |F_c||) / \sum |F_o|$; $R_w = [\sum w(|F_o| - |F_c|)^2 / \sum w F_o^2]^{1/2}$; $w = k[\sigma^2(F) + g(F)]$.

$\{[Mn(H_2O)_2\{\mu-H_2B(CHN_4)_2\}_2] \cdot 2 H_2O\}_\infty$ (**5**): A solution of 0.17 g (1.3 mmol) of anhydrous $MnCl_2$ in 15 ml of water was carefully overlaid in a test tube with a solution of 0.50 g (2.6 mmol) of the potassium salt of **4** in 20 ml of methanol. After 10 d the colorless solution was filtered from some precipitate and the solvent slowly allowed to evaporate from the filtrate at ambient temp. and pressure. The resulting crystalline material was washed once with 10 and twice with 5 ml of water to leave 0.30 g of large colorless crystals which analyzed as **5** (38% yield). Elemental analysis is included in Table 3. – IR (CsI): $\tilde{\nu} = 3350\text{ cm}^{-1}$ s, br (OH), 3145 s (CH), 2950 sh, 2485 s, (BH) 2460 m (BH), 2380–2200 w, 1805 w, br, 1700 w, br, 1625 w, br, 1490 m, 1480 s, 1392 m, 1377 m, 1287 m, 1245 w, 1190 s, 1169 w, 1159 s, 1140 m, 1110 s, 1042 m, 1005 s, 981 w, 905 m, 864 m, 745 w to m, 707 w to m, 622 s, br, 350 m, br.

$\{[M(H_2O)_2\{\mu-H_2B(CHN_4)_2\}_2] \cdot 2 H_2O\}_\infty$ [M = Fe (**6**), Co (**7**), Zn (**9**), Cd (**10**)]: A solution of 1.3 mmol of the transition metal salt [0.36 g of $FeSO_4 \cdot 7 H_2O$, 0.31 g of $CoCl_2 \cdot 6 H_2O$, 0.29 g of $Zn(O_2CCH_3)_2 \cdot 2 H_2O$, 0.26 g of $CdCl_2 \cdot H_2O$] in 15 ml of H_2O was carefully overlaid in a test tube with a solution of 0.50 g (2.6 mmol) of the potassium salt of **4** in 20 ml of water. Some amorphous material precipitated in this process. Slow diffusion of the starting compounds then led to the formation of **6**, **7**, **9**, and **10**, respectively, as analytically pure, well-shaped crystals. Except for the reaction with cadmium some gas evolution was also visible. Crystal growth usually started within 2 d, and the reaction and process of crystallization appeared to be concluded within 2 weeks. Yields, colors, melting points as well as the elemental analyses are compiled in Table 3. The infrared spectra of the compounds are almost identical, the Raman spectra very similar. The vibrational spectra for the zinc complex **9** are displayed in Figure 1. As an example the IR data are listed above for the manganese derivative **5**. – Raman: **7**: $\tilde{\nu} = 3151\text{ cm}^{-1}$ m, 2881 sh, 2457 s, 2440 sh, 1491 w, 1477 w, 1384 m, 1284 s, 1178 m, 1142 vw, 1049 m to s, 1018 w, 1005 vw, 705 w, 638 w, 626 w, 355 w, 269 w to m, 148 m, 109 s, 90 w. – **9**: $\tilde{\nu} = 3152\text{ cm}^{-1}$ m to s, 2482 sh, 2459 s, 2441 sh, 1491 w, 1479 vw, 1388 m, 1287 s, 1196 m, 1147 w, 1117 w to m, 1052 m to s, 1020 w, 979 w, 701 vw, 641 vw, 628 w, 356 vw, 270 w, 120 m, 78 sh, 65 s, 47 m. – **10**: $\tilde{\nu} = 3142\text{ cm}^{-1}$ m, 2481 sh, 2454 m, 2437 sh, 1492 w, 1478 vw, 1385 m to s, 1282 s, 1194 w, 1179 vw, 1145 vw, 1116 vw, 1049 m to s, 1017 vw, 977 vw, 704 vw, 639 vw, 626 w, 349 w, 261 w, 158 m, 107 w, 95 w, 79 w, 61 s.

$\{[Cu(NH_3)_2\{\mu-H_2B(CHN_4)_2\}_2]\}_\infty$ (**8**): A solution of 0.22 g (1.3 mmol) of $CuCl_2 \cdot 2 H_2O$ in 15 ml of water was carefully overlaid in a test tube with a solution of 0.50 g (2.6 mmol) of the potassium salt of **4** in 20 ml of water. No crystalline material, only a dark blue voluminous amorphous precipitate formed from which the supernatant clear solution was decanted after a month and the solid completely dissolved in concentrated aqueous ammonia (25%) to a clear deep blue solution. The solvent was slowly allowed to evaporate. During the process a dark blue-violet crystalline material formed together with some minor white, turquoise, and light blue crystals. The blue-violet fraction was manually separated and analyzed as **8** (yield 0.20 g, 38%). Elemental analysis see Table 3. – IR (KBr): $\tilde{\nu} = 3361\text{ cm}^{-1}$ w, 3342 w, 3152 m (CH), 2490 m, 2456 m (BH), 1617 w, 1500 w, 1486 m, 1470 w, 1397 w, 1288 w, 1246 vw, 1186 w, 1153 s, 1139 m, 1112 m, 1100 s, 1038 w, 1028 w, 1011 w, 976 w, 897 w, 876 vw, 742 vw, 705 m, 675 vw, 645 vw, 631 w, 621 w. – Raman: $\tilde{\nu} = 3153\text{ cm}^{-1}$ m, 2487 w, 2458 m, 1500 w, 1483 w, 1394 m, 1289 s, 1196 w, 1173 w, 1113 vw, 1097 s, 1007 w,

704 vw, 615 vw, 354 w, 271 w, 172 m, 132 m, 116 m, 107 s, 78 s, 66 m, 55 m, 50 m.

X-Ray Structure Determinations of 5–10: Syntex P2₁ four-circle diffractometer, ω scan ($0^\circ \leq 2\theta \leq 55^\circ$) for **5**, **7–10**; CAD4, Enraf-Nonius four-circle diffractometer, ω - 2θ scan ($6^\circ \leq 2\theta \leq 55^\circ$) for **6**; room temperature, Mo- K_α radiation ($\lambda = 0.71069\text{ \AA}$, graphite monochromator). Structure solution was performed by direct methods (SHELXS-86^[18]). Refinement: Full-matrix least-squares; all atomic positions including those of hydrogen atoms found and non-hydrogen atoms refined with anisotropic temperature factors (SHELX-76^[18]). Crystal data are listed in Table 4^[19].

* Dedicated to Professor Dr. Herbert Schumann on the occasion of his 60th birthday.

- [1] Reviews: S. Trofimenko, *Chem. Rev.* **1993**, *93*, 943–980; P. K. Byers, A. J. Canty, R. T. Honeyman, *Adv. Organomet. Chem.* **1992**, *34*, 1–65; K. Niedenzu, S. Trofimenko, *Topics Curr. Chem.* **1986**, *131*, 1–37; S. Trofimenko, *Progr. Inorg. Chem.* **1986**, *34*, 115–210.
- [2] S. Trofimenko, *J. Am. Chem. Soc.* **1967**, *89*, 3170–3177.
- [3] G. G. Lobbia, F. Bonati, P. Cecchi, *Synth. React. Inorg. Met.-Org. Chem.* **1991**, *21*, 1141–1151.
- [4] C. Janiak, *Chem. Ber.* **1994**, *127*, 1379–1385.
- [5] C. Janiak, L. Esser, *Z. Naturforsch., Teil B*, **1993**, *48*, 394–396.
- [6] C. Janiak, *J. Chem. Soc., Chem. Commun.* **1994**, 545–547; C. Janiak, T. G. Scharmann, H. Hemling, D. Lentz, J. Pickardt, *Chem. Ber.* **1995**, *128*, 235–244.
- [7] C. Janiak, H. Hemling, *J. Chem. Soc., Dalton Trans.* **1994**, 2947–2952.
- [8] M. Fujita, Y. J. Kwon, S. Washizu, K. Ogura, *J. Am. Chem. Soc.* **1994**, *116*, 1151–1152; A. M. A. Ibrahim, T. M. Soliman, S. E. H. Etaiw, R. D. Fischer, *J. Organomet. Chem.* **1994**, *468*, 93–98.
- [9] S. Decurtins, H. W. Schmalke, H. R. Oswald, A. Linden, J. Enslin, P. Gütllich, A. Hauser, *Inorg. Chim. Acta* **1994**, *214*, 65–73; J. J. Borrás-Almenar, E. Coronado, C. J. Gómez-García, L. Ouahab, *Angew. Chem.* **1993**, *105*, 637–639; *Angew. Chem. Int. Ed. Engl.* **1993**, *32*, 561–563; G. De Munno, M. Julve, F. Nicolo, F. Lloret, J. Faus, R. Ruiz, E. Sinn, *Angew. Chem.* **1993**, *105*, 588–590; *Angew. Chem. Int. Ed. Engl.* **1993**, *32*, 613–615.
- [10] R. Robson, B. F. Abrahams, S. R. Batten, R. W. Gable, B. F. Hoskins, J. Liu, *Supramolecular Architecture, Synthetic Control in Thin Films and Solids* (ACS Symposium Series 499) (Ed.: T. Bein), American Chemical Society, Washington, DC, **1992**, p. 256–273.
- [11] S. B. Copp, S. Subramanian, M. J. Zaworotko, *Angew. Chem.* **1993**, *105*, 755–758; *Angew. Chem. Int. Ed. Engl.* **1993**, *32*, 706–708; *J. Chem. Soc., Chem. Commun.* **1993**, 1078–1088.
- [12] A. L. Spek, *PLATON-93 and PLUTON-92 graphics program*, University of Utrecht, The Netherlands, **1993** and **1992**, respectively; A. L. Spek, *Acta Crystallogr., Sect. A*, **1990**, *46*, C34.
- [13] J. E. Huheey, *Inorganic Chemistry*, 3rd ed., Harper & Row, New York, **1983**, p. 388.
- [14] C. Lopez, R. M. Claramunt, D. Sanz, C. F. Foces, F. H. Cano, R. Faure, E. Cayon, J. Elguero, *Inorg. Chim. Acta* **1990**, *176*, 195–204.
- [15] G. J. Palenik, *Acta Crystallogr.* **1963**, *16*, 596–600; J. H. Bryden, *ibid.* **1958**, *11*, 31–37; G. B. Ansell, *J. Chem. Soc., Dalton Trans.* **1973**, 371–374, and references therein.
- [16] A. Weiss, H. Witte, *Magnetochemie*, Verlag Chemie, Weinheim, **1973**.
- [17] F. E. Mabbs, D. J. Machin, *Magnetism and Transition Metal Complexes*, Chapman and Hall, London, **1973**.
- [18] G. M. Sheldrick, *SHELX-76, Program for Crystal Structure Determination*, Cambridge, **1976**; *SHELXS-86, Program for Crystal Structure Solution*, Göttingen, **1986**.
- [19] Further details of the crystal structure determinations are available on request from the Fachinformationszentrum Karlsruhe, Gesellschaft für wissenschaftlich-technische Information mbH, D-76344 Eggenstein-Leopoldshafen, on quoting the depository number CSD-58 782, the authors, and the journal citation.

[390/94]